Available online at www.sciencedirect.com

ScienceDirect

Ceramics International 38 (2012) 45–53

CERAMICS INTERNATIONAL

www.elsevier.com/locate/ceramint

# Densification of additive-free polycrystalline β-SiC by spark-plasma sintering

Ana Lara [a], Angel L. Ortiz [b,*], Antonio Muñoz [a], Arturo Domínguez-Rodríguez [a]

[a] *Departamento de Física de la Materia Condensada, Facultad de Física, Universidad de Sevilla, 41012 Sevilla, Spain*
[b] *Departamento de Ingeniería Mecánica, Energética y de los Materiales, Universidad de Extremadura, Badajoz 06071, Spain*

Received 7 February 2011; received in revised form 15 June 2011; accepted 17 June 2011

**Abstract**

Additive-free β-SiC nanopowders were densified by spark-plasma sintering in the temperature range 1650–2200 °C, holding time 1–30 min, and pressure 50–150 MPa. The starting nanopowder was further refined and mechanically activated by ball milling in order to promote densification. In a detailed parametric study, temperature, holding time, and/or pressure were varied to investigate their effect on the densification and grain growth during sintering. High densifications were obtained for temperatures greater than 1800 °C. Full densification (98.0 ± 0.6%) was reached at a sintering temperature of 2100 °C. Depending on the sintering conditions, nanostructured materials can be produced with grain sizes between 90 and 100 nm, and microstructured materials with grain sizes between 0.22 and 2.39 μm. Pressure has a major effect on the grain size, it being necessary to use a pressure of 150 MPa to obtain nanostructured materials.

*Keywords:* Spark-plasma sintering; SiC; Nanostructured ceramics; Densification

## 1. Introduction

Its excellent mechanical properties at high and low temperatures make SiC a very interesting advanced ceramic. With its resistance to erosion, oxidation, and high temperatures, its thermal and chemical stability, and its exceptional hardness, it has many industrial applications [1]. Since materials with grain sizes in the nanoscale (less than 100 nm) have greater hardness and fracture strength, there has been interest in the processing of nanostructured SiC, for which one requires suitable prior production and preparation of a nanocrystalline starting powder.

One of the greatest drawbacks in the manufacture of nanostructured SiC is the difficulty in sintering dense, nano-grained samples without the use of additives. This is because the covalent nature of the Si–C bonds and the low self-diffusion coefficients require very high sintering temperatures and pressures. Liquid-phase sintering (LPS) allows densification of SiC at temperatures close to 1900 °C without the use of external pressures. These temperatures are much lower than the close to 2200 °C required by the conventional solid-state sintering. The disadvantage of LPS, however, is the inevitable formation of a residual intergranular phase. Can et al. [2] describe liquid-phase densification of SiC by hot-isostatic pressing using proportions of additives ($Al_2O_3/Y_2O_3$) ranging from 4:1 to 2:1. They extrapolate that, for densities approaching 100%, it would be necessary to use quantities of ($Al_2O_3/Y_2O_3$) additives representing about 10 wt%. Different proportions of each of the $Al_2O_3$ and $Y_2O_3$ additives, or other rare-earth oxides, result in different phases at the grain boundaries (aluminates, silicates, garnet, etc.), which might determine the mechanical properties of the sintered material. Shinoda et al. [3] have sintered SiC by hot-pressing using a nanocrystalline starting powder (average grain size 30 nm) containing 3.5 wt% of free carbon. This powder was sintered with and without boron doping (between 1 and 10 wt%) at a pressure of 980 MPa and a temperature of 1600 °C. In both cases, materials were obtained with densities of $3.12\ g\ cm^{-3}$ (97.1% relative density), with the mean grain size being 200 nm for the doped and only 30 nm for the non-doped samples. One deduces from this that it may be possible to obtain nanostructured SiC materials by hot-pressing with practically no grain growth and densities close to 97%, but that it would require the use of ultra-high pressures.

---

* Corresponding author. Tel.: +34 924289600x86726; fax: +34 924289601.
*E-mail addresses:* alortiz@materiales.unex.es, alortiz@unex.es
(A.L. Ortiz).

0272-8842/$36.00 © 2011 Elsevier Ltd and Techna Group S.r.l. All rights reserved.
doi:10.1016/j.ceramint.2011.06.036

Microwave sintering requires lower temperatures than conventional sintering, and also allows shorter sintering times. A problem is, however, that most ceramic materials do not absorb microwaves at 2.45 GHz (the commonest frequency in these devices), so that it again becomes necessary to add some absorbant such as carbon to improve sintering [4] or to use a secondary source of heating [5]. In the specific case of SiC, conductivity increases with temperature [6], although it is necessary to use an inert atmosphere to prevent the formation of oxides that behave as insulators [7], bearing in mind that argon atmospheres cannot be used in the commonest microwave devices. Neither is it possible to use nitrogen because $Si_3N_4$ will be formed on the green body surface and will act as an insulator and impede the microwave sintering. So far, it has only been possible to process SiC by microwaves via LPS, with the concomitant use of large amounts of additives [8]. Therefore, microwave sintering is not an option if one wishes to fabricate SiC free of secondary phases.

In the present work we used what we believe to be the most appropriate technique for this purpose, that is, spark-plasma sintering (SPS). Currently, improved powder processing technology has made high purity nanocrystalline powders commercially available. This improvement, coupled with advances in sintering techniques, allows one to obtain polycrystalline nanostructured ceramic materials. The technique of SPS consists of applying pressure to a starting powder while a pulsed electric current is passed through the die, and through the powder if it is electrically conductive, to heat the powder compact directly by the Joule effect. This technique has certain advantages over conventional sintering or hot-pressing since it yields higher densities at lower temperatures and shorter times without the use of additives, thus obtaining secondary phase free materials with smaller grain sizes. With the SPS technique, nanostructured SiC materials have been obtained with densities of 98% and grain sizes of 20–50 nm without the use of additives or high pressures [9]. In that work, a SiC powder obtained by mechanosynthesis was used for sintering, and the processing parameters were 40 MPa, 1900 °C, and 10 min. However, the use of the same sintering conditions but with a commercial nanocrystalline starting powder not activated by milling yielded a material of only 78% density. Furthermore, during the sintering, phase changes were observed in the SiC sintered from the powder prepared by mechanosynthesis. These phase changes may have been the result of mass transport phenomena which occur as the structure of the SiC is rearranged during the rapid densification. No such changes were observed in the case of the SiC commercial powder [9]. For this reason, it seems reasonable to mechanically activate the powder by milling techniques in order to facilitate the subsequent sintering. Simultaneous studies to the foregoing conducted by Yamamoto et al. [10] again highlighted the importance of order–disorder transformations in the process of densification. Based on the same experiments as were reported by Ohyanagi and Yamamoto [9], it was concluded that a positive correlation exists between the densification of the SiC and the disappearance of disorder, understanding by disorder the polytypism (different stacking sequences) in the SiC starting powder obtained by high-energy milling.

Subsequently, Guillard et al. [11] sintered SiC by SPS without the use of additives in the temperature range of 1750–1850 °C at a pressure of 75 MPa, and sintering times between 1 and 10 min. A commercial SiC starting powder was used, and the materials obtained had densifications of up to 92% and a mean grain size of 2 μm under the sintering conditions of 1850 °C, 5 min, and 75 MPa. It was concluded that grain growth was strongly related to the sintering temperature, and to a lesser extent to the sintering time. The densification was found to improve and the grain growth to reduce if the pressure was applied after a certain temperature had been reached (in the experiments, the pressure increase was applied at a temperature of 1000 °C), instead of applying all the pressure before starting the heating.

Zhang et al. [12] sintered SiC by SPS from an agglomerated powder with a particle size between 0.5 and 1 μm, and an agglomerate size of 80 μm. The sintering parameters were: pressures between 1 and 50 MPa, temperatures between 800 °C and 1860 °C with a heating ramp of 150 $°C\,min^{-1}$, and sintering time of 5 min. They confirmed that no sintering occurred for temperatures below 1700 °C. The samples were characterized by scanning electron microscopy, finding a positive correlation between processing temperature and the resulting density. Values of densification up to 98.5% were attained with the agglomerated powder, but under the same conditions the non-agglomerated powder densification was only 80.2%. With respect to the grain size, there was a growth from 1.25 to 2.05 μm with increasing sintering temperature from 1700 °C to 1860 °C.

In the present work, the sintering process was facilitated by pre-treating the starting powder by ball milling in a centrifugal mill. Milling mechanically activates the powder particles and reduces their size, thereby improving the subsequent sintering. In recent years, such milling has aroused considerable scientific interest in the materials science community. Yang and Shaw [13] studied the synthesis of nanocrystalline SiC using high-energy ball milling, using an attrition mill into which silicon and graphite were introduced and then milled at different speeds using WC balls. The result was the production of nanocrystalline SiC powders with a crystallite size of less than 25 nm. They also noted that increasing the speed of milling increased its efficacy while introducing internal stresses into the crystal lattice. Similarly, increasing the milling time reduced the crystallite size and increased the density of defects in the crystal lattice.

Later, Yang et al. [14] used high resolution transmission electron microscopy to study at the atomic scale the synthesis of SiC by milling. They observed the formation of amorphous graphite, amorphous Si, and nanocrystalline Si with many defects during milling at a stage prior to synthesis. Subsequently, the C atoms began to replace the Si atoms, resulting in the formation of SiC.

Chaira and Mishra [15] describe the synthesis and characterization of SiC obtained by milling in a planetary mill. They ran the milling for 40 h with two sizes of balls (6 and 12 mm in diameter), and took powder samples at various intervals for analysis. They observed that the powder obtained with the larger diameter balls had a smaller crystallite size

(10 nm) than with the smaller balls (40 nm). Both powders presented agglomerates that the authors tried to eliminate through the use of dispersants, obtaining a powder with 20% of particles smaller than 1 μm. They also noted that during the first 20 h of milling there was an increase in the lattice stresses and a decrease in crystallite size, and that from that time onwards there began the synthesis of the SiC powder and the lattice stresses decreased.

Subsequently, Abderrazak and Abdellaoui [16] obtained a nanocrystalline SiC powder after milling Si and C powders using a planetary mill with 15 mm diameter balls. The reaction occurred gradually, being complete after 15 h. The crystallite size measured by X-ray diffraction was 4 nm. Ghosh and Pradhan [17] obtained nanocrystalline SiC powder by high-energy milling of Si and C at room temperature in an inert atmosphere. The X-ray diffraction analysis of the milled powder showed that the crystallite size declined after 3 h of milling, and that the lattice stresses increased up to 5 h when the synthesis reaction began. The reaction was complete at times exceeding 15 h.

Ohyanagi and Yamamoto [9] demonstrated that there was a clear improvement in the density and microstructure of the samples when using SiC powders obtained by mechanosynthesis instead of commercial powders. They synthesized nanocrystalline SiC powder by high-energy milling of Si and C powder using 10 mm balls, obtaining crystallites with sizes between 5 and 20 nm and agglomerates of 50–150 nm. Yamamoto et al. [10] showed by X-ray diffraction that the milling introduces defects into the crystal lattice, and that these defects contribute to improving the subsequent densification of the material.

In the present work, we studied the effect of different SPS processing parameters (heating rate, and the sintering temperature, time, and pressure) with the goal of obtaining a highly densified SiC material with nanometric grain size. The parametric study involves more than 25 different SPS conditions. It is only by carrying out this detailed parametric study that the SPS processing window of nanostructured SiC can be identified. The aim is to use SPS to densify additive-free SiC so as to be able to evaluate in the future the intrinsic properties of this advanced ceramic.

## 2. Experimental procedure

The starting material was high purity β-SiC powder (Sumitomo Osaka Cement Co. Ltd.) fabricated by plasma-enhanced chemical vapour deposition. The mean grain size was 30 nm. This starting powder includes small amounts of impurities of N (0.0047 wt%) and O (0.3428 wt%). The crystalline characterization of this powder was performed by X-ray diffraction (XRD; Model D8-Advance, Bruker AXS) with Cu-Kα radiation. The generator settings were 40 kV and 35 mA. The XRD data were acquired over a $2\theta$ range of 15–95° using the step-scan mode with 0.02° steps and 15 s intervals. The mean grain size was determined by field-emission scanning electron microscopy (FE-SEM; Model Hitachi S5200). The particle size distribution (agglomerates) in the powder was measured before and after milling (Model NanoZetaSizer, Malvern Instruments).

To improve densification and avoid grain growth in so far as possible during sintering, the starting powder was milled in a centrifugal ball mill (Model S-100, Retsch) under ambient conditions. The ball-to-powder weight ratio was 40:1, the canister was filled to 1/3, and the milling speed was 400 rpm. The mill canister was made of WC and the balls of SiC to minimize contamination of the powder. The ball-milling time was varied in the range of 0.5–24 h to impact different degrees of milling intensity. The ball-milled β-SiC nanopowders were analyzed by XRD to determine the evolution of the crystallite sizes and the internal stresses with ball-milling time from the broadening of the XRD peaks [18–20].

The powders were densified in vacuum without the use of additives in an SPS apparatus (Model 515S, SPS Syntex Inc.). The process involves a high pulsed DC current (20 V, 0–1500 A) with the simultaneous application of uniaxial pressure. The scheme of the device is shown in Fig. 1. The powder samples, wrapped in graphite foil of 0.4 mm thickness, were put individually into a cylindrical graphite die of inner diameter 10 mm and outer diameter 40 mm. The trial pressure (between 50 and 150 MPa) was applied through the top and bottom punches, each having an approximate diameter of 9.2 mm and a length of 10 mm. The powders were heated at a ramp rate between 100 °C $\text{min}^{-1}$ and 200 °C $\text{min}^{-1}$ up to the target temperature in the range of 1650–2200 °C, and then held at that temperature for 1–30 min. The experimental parameters of temperature, vacuum, applied pressure, current, stress, and sample shrinkage were monitored throughout the densification cycle. Temperatures were measured by an optical pyrometer focused on the die surface. The sintered samples were allowed to cool to room temperature by turning off the power. They were in the form of a disk of about 10 mm diameter and 3 mm thickness. The relative bulk densities of these samples were measured based on the Archimedes principle.

The microstructure features – pore distributions and grain size and morphology – were studied using FE-SEM. Prior to observation, the sintered samples were polished to a 3-μm finish with diamond paste, and then plasma etched ($CF_4$ and $O_2$

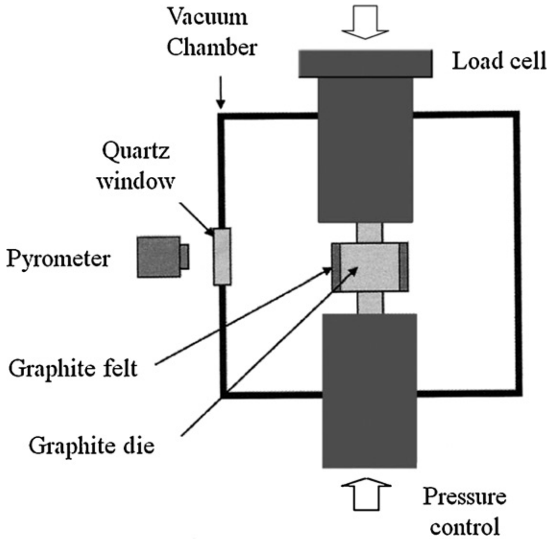

Fig. 1. Schematic diagram of the spark-plasma sintering (SPS) system.

in the ratio 1:6) for 5 h (Model Plasma Asher K1050X, Emitech). The microstructural information was determined using a videoplan image analyzer (Model Videoplan MOP 30, Kontron Electronik GmbH.).

## 3. Results and discussion

Fig. 2 shows the XRD pattern of the commercial starting powder in which one observes that the SiC is of type β (i.e., polytype 3C) with planar defects (i.e., stacking faults and microtwins), and Fig. 3 is a representative FE-SEM image of that SiC starting powder showing an average grain size of about 30 nm. The two results confirm the supplier's specifications.

Fig. 4 is a comparison of a region of the XRD patterns of the β-SiC powder before and after ball milling for 3 h. One observes clearly the broadening of the peaks following milling, reflecting crystallite size refinement and/or the introduction of defects into the crystal lattice [21–23]. No variation in the relative integrated intensities of the β-SiC peaks was observed during the examination of the entire XRD patterns. To identify the causes of the peak broadening, Voigt functions were fitted to the XRD peaks before and after milling, finding that the integral breadth of the Lorentz component increased with milling time but integral breadth of the Gaussian component did not. These observations indicate that the cause of peak broadening is the reduction of crystallite size, not the introduction of defects into the crystal lattice, and therefore reveal that ball-milling has refined the nano-grain size of the β-SiC starting powder together with its most likely mechanical activation via the introduction of surface defects in the nano-grains. The Voigt function fits were used to calculate the mean crystallite size ($D$) using the variance method according to the expression [18]:

$$D = \frac{108.81\lambda}{\pi(\beta_{L,h} - \beta_{L,g})\cos\theta_0}$$

where $\beta_L$ is the integral breadth of the Lorentz component of the Voigt function, $\theta_0$ is the Bragg angle, $\lambda$ is the wavelength of the X-ray incident beam, and the subscripts $g$ and $h$ refer to a coarse SiC powder and the milled powder, respectively. Fig. 5 shows the estimated crystallite sizes as a function of milling time. One observes in the figure that the crystallite size initially decreases with milling time to stabilize at around 10 nm after 8 h, suggesting that prolonged milling will fail to significantly further reduce the crystallite size. Thus, the powder milled for 8 h will be the one used for the subsequent SPS studies.

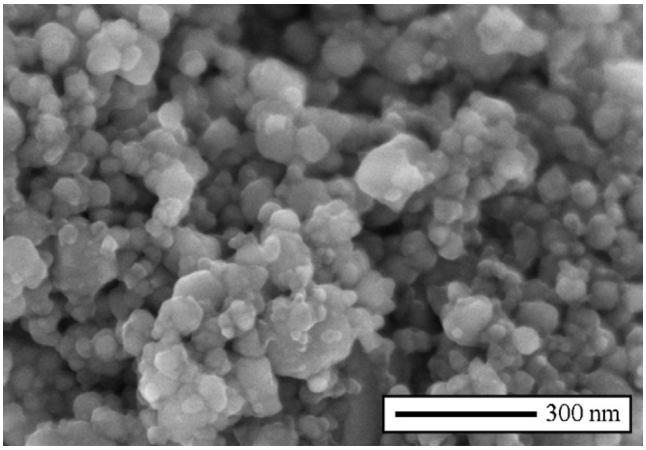

Fig. 3. FE-SEM image of the SiC starting powder.

To obtain dense materials with small grain size, not only the starting powder crystallite size is important but also whether or not there exist agglomerates, and if so, their mean size. Fig. 6 shows the results of measurements of the particle (agglomerate) size distribution in the powder before and after milling for 8 h. One sees that while the milling completely eliminates the larger agglomerates, there remains a major presence of smaller agglomerates.

Table 1 lists the SPS parameters (temperature, heating rate, sintering time, and pressure) used to fabricate various additive-free SiC samples, together with the characteristics of the resulting materials. As can be seen, sintering was performed for temperatures between 1650 °C and 2200 °C, pressures between

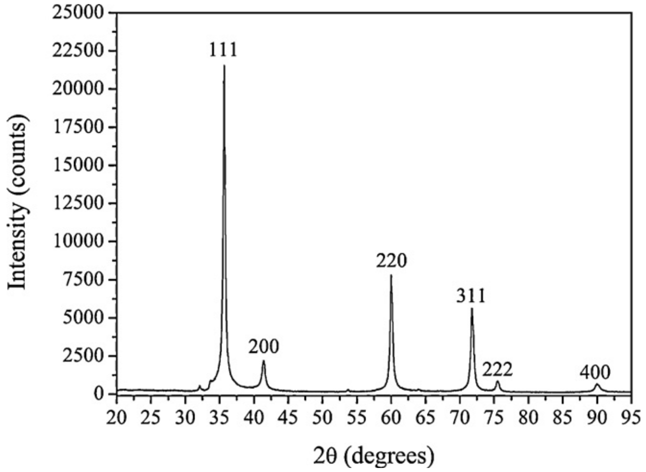

Fig. 2. XRD pattern of the SiC starting powder.

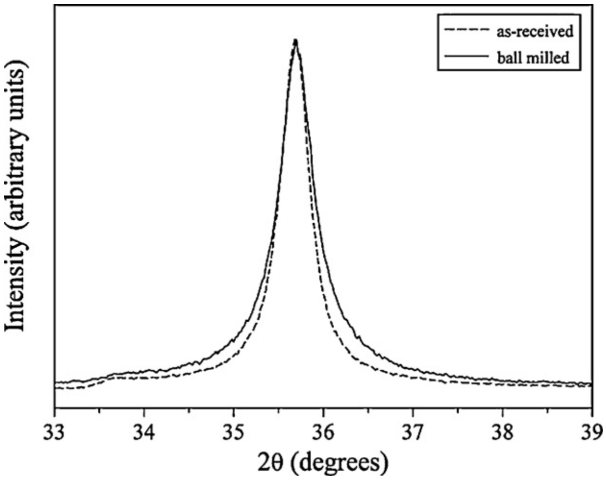

Fig. 4. 111-XRD peak for the as-received β-SiC and the 3-h ball-milled β-SiC after correction for instrumental shifts.

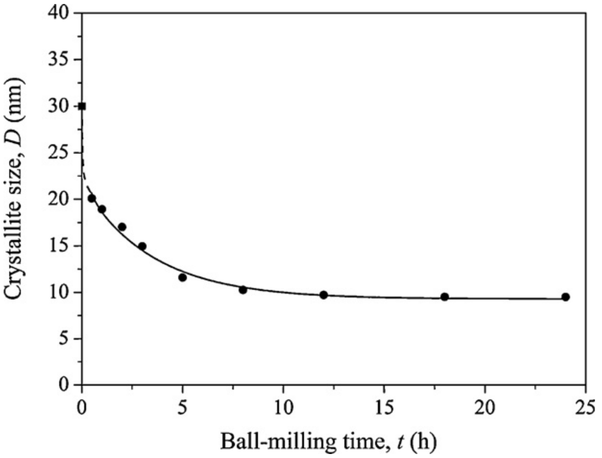

Fig. 5. The mean crystallite size of β-SiC as measured by XRD versus ball-milling time (solid disc points). The crystallite size of the as-received β-SiC powder measured by FE-SEM is included for comparison (solid square point).

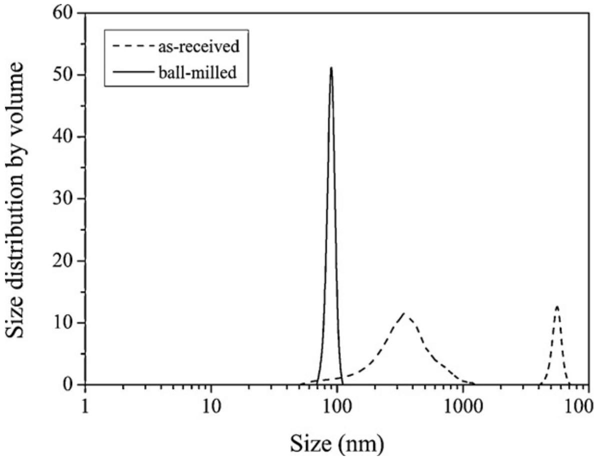

Fig. 6. Particle size distribution of the β-SiC powder before and after milling.

50 and 150 MPa, sintering times between 1 and 30 min, and heating rates between 100 and 200 °C min$^{-1}$. With these SPS conditions, XRD indicated that the sintered materials are formed of β-SiC with lower density of planar defects relative to the starting and ball-milled powders, thus revealing the occurrence of structural ordering of SiC during SPS in concordance with previous observations [9]. It can also be seen in Table 1 that at temperatures below 1800 °C densification was incomplete, it being necessary to attain temperatures between 1800 °C and 2200 °C to achieve densification of the material greater than 90%. One notes that at a pressure of 150 MPa one obtains nanostructured materials which, however, contain a few grains of micrometre size (Fig. 7).

For temperatures above 1900 °C there was a gradual increase of densification with temperature, eventually reaching densifications of 98%. Ohyanagi and Yamamoto [9] used the same commercial powder than employed here but without the milling pre-treatment. The greatest densification they obtained

Table 1
Sintering parameters and microstructural characteristics of the materials obtained with the different SPS conditions.

| Sample | *T* (°C) | Pressure (MPa) | Time (min) | Heating rate (°C min$^{-1}$) | Relative density ± 0.6 (%) | Grain size (μm) | Form factor | Observations |
|---|---|---|---|---|---|---|---|---|
| S-1 | 1650 | 150 | 5 | 200 | 78.0 | | | Not sintered |
| S-2 | 1800 | 70 | 10 | | 80.0 | | | Partially sintered |
| S-3 | | 100 | 5 | | 87.9 | 0.44 ± 0.14 | 0.64 ± 0.14 | |
| S-4 | | | 10 | | 87.9 | 0.84 ± 0.22 | 0.64 ± 0.14 | |
| S-5 | | 150 | 5 | | 90.0 | 0.105 ± 0.028 | 0.53 ± 0.11 | Nanometric but inhomogeneous |
| S-6 | 1850 | 70 | 30 | 100 | 85.1 | 1.07 ± 0.24 | 0.67 ± 0.14 | |
| S-7 | 1875 | 70 | 30 | | 85.4 | 1.38 ± 0.31 | 0.62 ± 0.12 | |
| S-8 | 1900 | 70 | 15 | | 86.6 | 1.49 ± 0.33 | 0.61 ± 0.14 | |
| S-9 | | | 30 | | 87.3 | 1.67 ± 0.36 | 0.66 ± 0.13 | |
| S-10 | | 100 | 5 | 200 | 90.7 | 0.67 ± 0.19 | 0.65 ± 0.14 | |
| S-11 | | | 15 | 200 | 92.0 | 0.73 ± 0.18 | 0.66 ± 0.11 | |
| S-12 | | 150 | 5 | | 91.0 | 0.095 ± 0.025 | 0.54 ± 0.12 | Nanometric but inhomogeneous |
| S-13 | 1950 | 70 | 30 | 100 | 88.7 | 1.95 ± 0.34 | 0.65 ± 0.09 | |
| S-14 | | 100 | 10 | 200 | 91.6 | 0.77 ± 0.21 | 0.66 ± 0.14 | |
| S-15 | | 150 | 5 | 200 | 91 | 0.091 ± 0.025 | 0.52 ± 0.13 | Nanometric but inhomogeneous |
| S-16 | | | 7 | | 94.0 | 0.99 ± 0.25 | 0.68 ± 0.14 | |
| S-17 | 2000 | 70 | 30 | 100 | 89.2 | 1.91 ± 0.34 | 0.90 ± 0.18 | |
| S-18 | 2050 | 70 | 30 | | 93.4 | 2.08 ± 0.32 | 0.92 ± 0.16 | |
| S-19 | 2075 | 70 | 30 | | 93.2 | 2.15 ± 0.31 | 0.67 ± 0.15 | |
| S-20 | 2100 | 70 | 30 | | 98.0 | 2.39 ± 0.35 | 0.63 ± 0.17 | |
| S-21 | | 100 | 5 | 200 | 91.0 | 0.97 ± 0.24 | 0.50 ± 0.11 | |
| S-22 | | 150 | 5 | | 92.0 | 0.098 ± 0.024 | 0.53 ± 0.12 | Nanometric but inhomogeneous |
| S-23 | 2150 | 100 | 3 | | 90.0 | 0.85 ± 0.19 | 0.64 ± 0.14 | |
| S-24 | 2200 | 100 | 0 | 200 | 89.0 | 2.2 ± 0.33 | 0.89 ± 0.19 | |
| S-25 | | | 0 | | 90.0 | 1.72 ± 0.29 | 0.92 ± 0.18 | |
| S-26 | | | 3 | | 94.3 | 0.79 ± 0.16 | 0.60 ± 0.12 | |
| S-27 | | 150 | 3 | 200 | 94.0 | 1.20 ± 0.23 | 0.63 ± 0.12 | |

Theoretical density of β-SiC = 3.21 g cm$^{-3}$. A blank space in the Table implies that the previous number in the column applies.

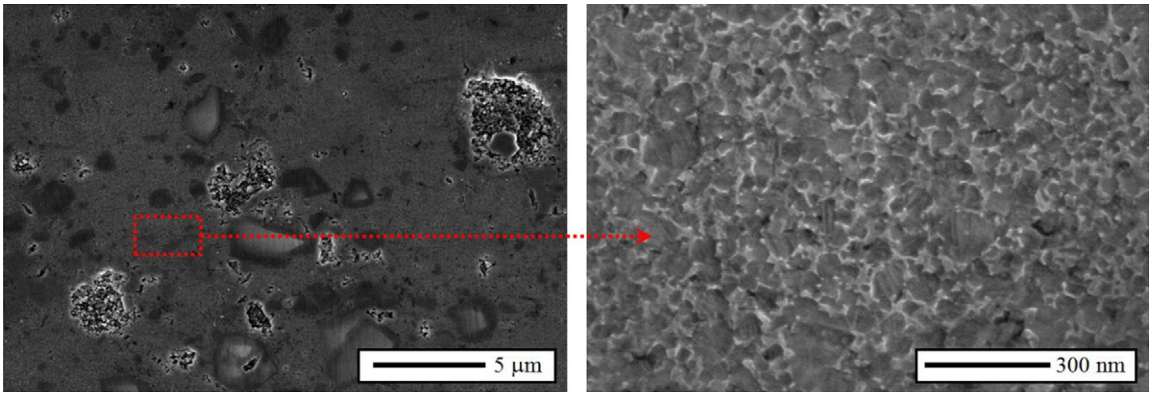

Fig. 7. FE-SEM micrograph of SiC sintered at 1950 °C for 5 min with 150 MPa (S-15 in Table 1).

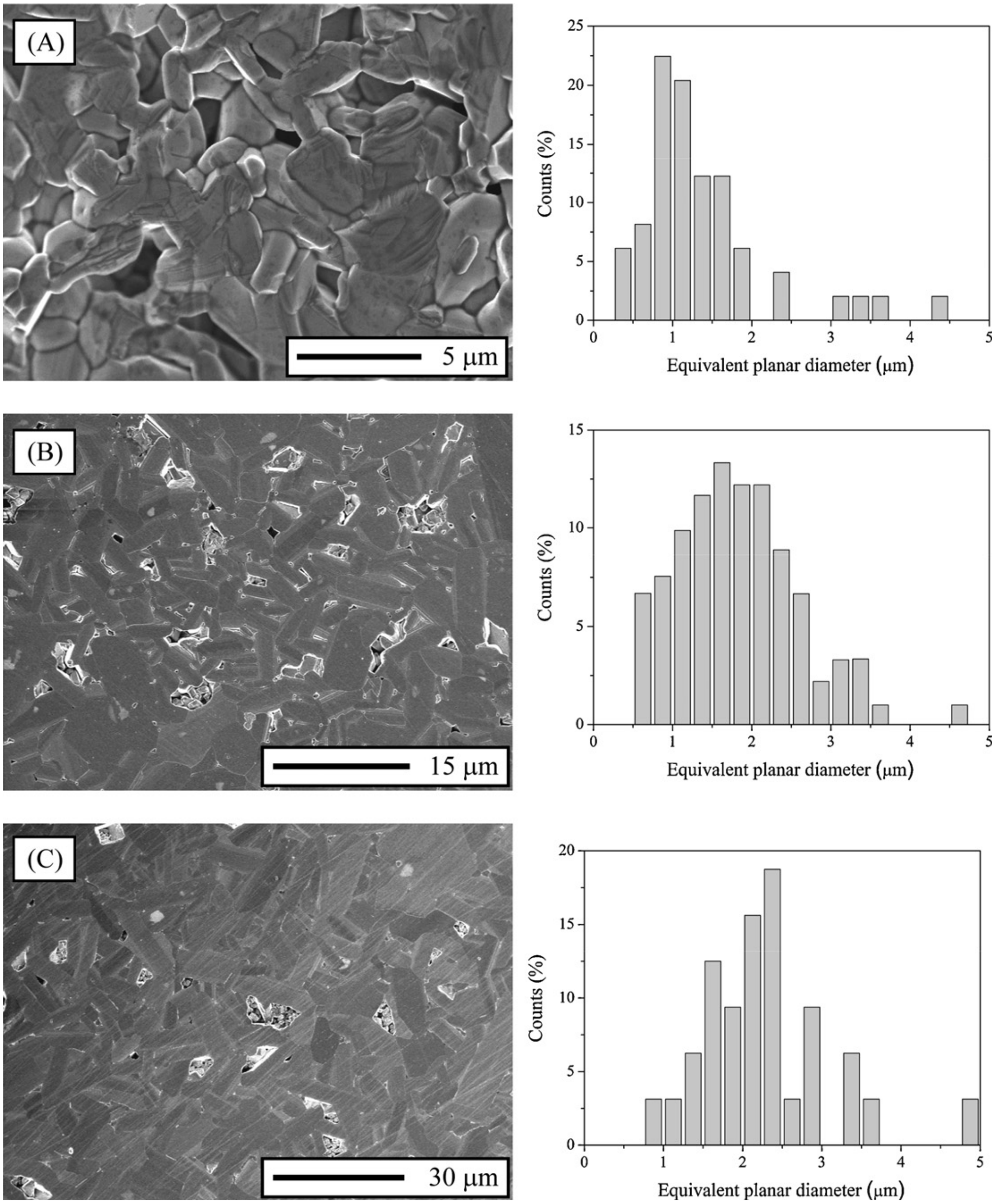

Fig. 8. FE-SEM micrographs and grain size histograms of SiC sintered at 70 MPa for 30 min with a heating ramp of 100 °C $\text{min}^{-1}$. Sintering temperature was (a) 1875 °C (S-7 in Table 1), (b) 2050 °C (S-18 in Table 1), and (c) 2100 °C (S-20 in Table 1).

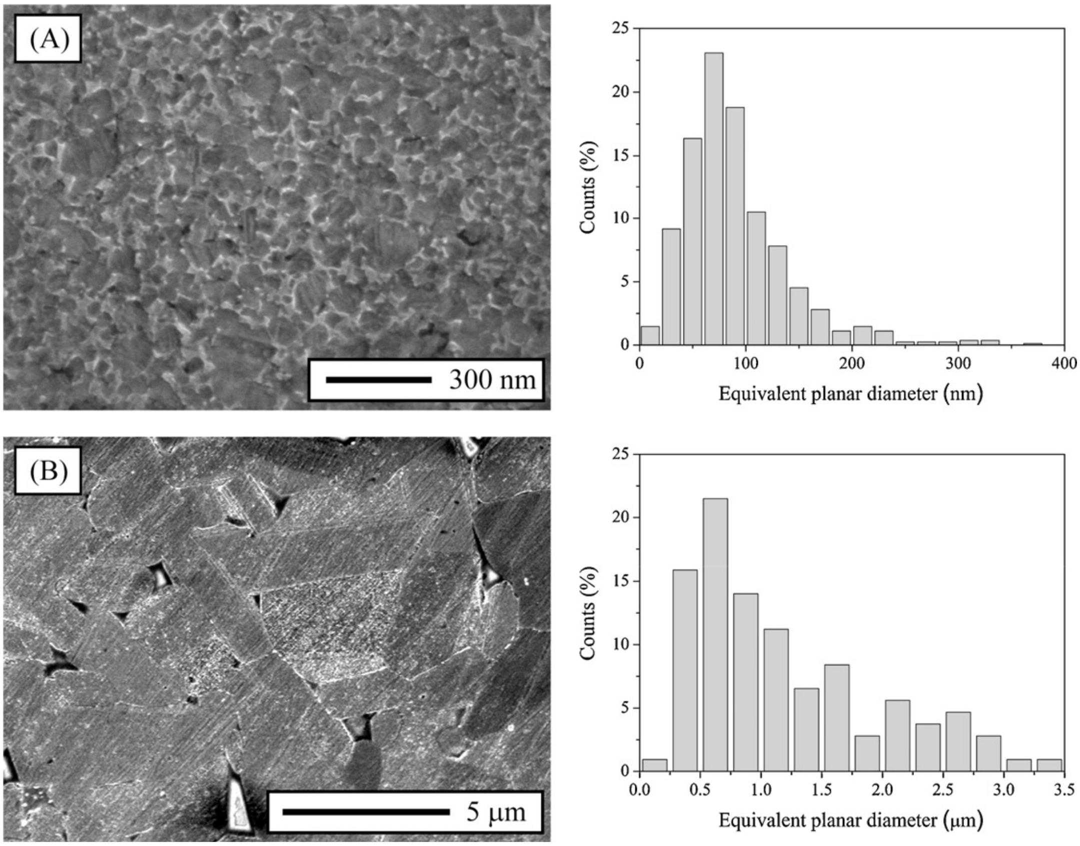

Fig. 9. FE-SEM micrographs and grain size histograms of SiC sintered at 150 MPa with a heating ramp of 200 °C $min^{-1}$: (a) $T$ = 1950 °C, $t$ = 5 min (S-15); and (b) $T$ = 2200 °C, $t$ = 3 min (S-27).

was 80% at 1900 °C, well below the value obtained in the present work at the same temperature. There would hence appear to be an improvement in sintering as a result of the refinement and mechanical activation of the SiC starting powder via ball milling.

It can also be noted in Table 1 that, depending on the sintering conditions, one can attain densifications of up to 98.0 ± 0.6%, and grain sizes between 0.091 and 2.39 μm. In general, densification improves with increasing temperature and sintering time. Fig. 8 shows micrographs corresponding to materials sintered at 70 MPa for 30 min with a heating ramp of 100 °C $min^{-1}$, and temperatures between 1875 °C and 2100 °C. Together with each micrograph is shown the corresponding histogram of the grain size distribution. As expected, there was an increase of grain size and a decrease of porosity with increasing sintering temperature. Similarly, Fig. 9 shows the micrographs corresponding to materials sintered at 150 MPa for 3–5 min with a heating ramp of 200 °C $min^{-1}$, and temperatures of 1950 °C and 2200 °C. One observes that to obtain nanostructured materials it is necessary to use high pressures (at least 150 MPa), short sintering times (5 min), and temperatures that are not excessively high (below 2200 °C). With these conditions, the densifications obtained were only around 90%. Pressures of 150 MPa yielded several nanostructured materials, but they were inhomogeneous in the sense that they contained some micrometre-sized grains. This was because, while the powder grain size was nanometric and the sintering conditions were appropriate, the powder contained agglomerates that were not totally eliminated by the milling or by the effect of pressure. During sintering, these agglomerates resulted in these micrometre-sized grains. Fig. 10 is a micrograph of a homogeneous, micrometre-grained material. Some of the grains in turns contain smaller grains in their interior, showing that grain growth is taking place from agglomerates in the starting powder. The application of pressure has direct effects on the particle redistribution, the

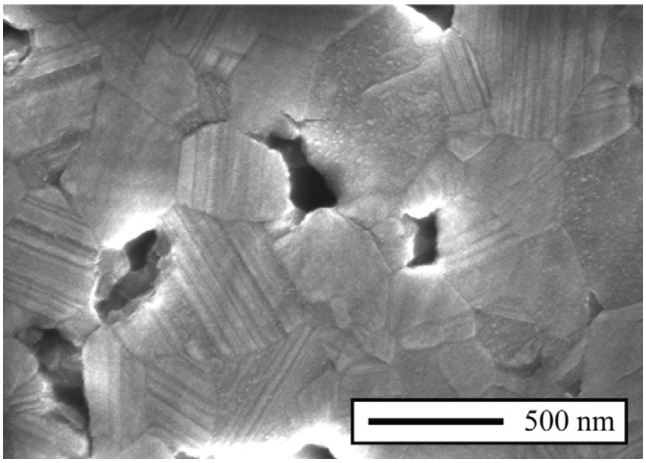

Fig. 10. FE-SEM micrograph of the sample sintered at 2200 °C for 3 min with 100 MPa, with a densification of 94.3% (S-26 in Table 1).

elimination of pores, and the destruction of agglomerates, particularly in the case of nanopowders [24]. In the micrographs of Fig. 7 of a sample sintered at a pressure of 150 MPa, one observes large areas of nanometre-sized grains that correspond to zones in which the pressure has had the effect of destroying the agglomerates.

At lower pressures, the materials are homogeneous but of micrometric grain size. In general, one observes a gradual increase in densification with temperature, and a decrease in grain size with pressure (Table 1). This may be due to the applied pressure breaking up the agglomerates in the powder. With respect to the sintering time, at equal temperatures and pressures or even under higher pressures an increase of sintering time leads to greater final densities, but with the drawback of increasing grain size.

## 4. Conclusions

A detailed parametric study has been performed to optimize the SPS conditions for the additive-free densification of SiC nanopowder. The following conclusions can be drawn from the results:

(1) Ball milling refines the crystal size of β-SiC nanopowder, yielding a mean crystallite size of 10 nm after 8 h. This refinement of the crystallite size and the mechanical activation resulting from the milling favoured the subsequent SPS densification of the nanopowder.

(2) With the SPS conditions employed in the present work – milling, heating rate, pressure, and sintering time – high densifications (i.e., 90% or greater) were achieved at temperatures above 1800 °C.

(3) Densification increased with temperature and sintering time, reaching 97.5 ± 0.6% of the theoretical density at 2100 °C. There was a progressive increase in densification from 80.0% to 97.5% with increasing sintering temperature. These densifications are better than those reported in the literature for materials sintered from the same commercial SiC starting nanopowder but without the milling pre-treatment. Similarly, increased sintering pressure contributed to improving the densification, although, while the effect was important at low temperatures, it was less so when the sintering temperature approached or exceeded 2200 °C.

(4) Materials were obtained with grain sizes that were nanometric (between 90 and 100 nm) and submicrometric and micrometric (between 0.22 and 2.39 μm). There was a major effect of pressure on grain size, with the nanometric grain size only being achieved with the application of a high pressure (150 MPa). This was possibly due to the pressure destroying agglomerates present in the nanocrystalline powder. Obtaining nanostructured materials also requires the use of short sintering times and temperatures that are not excessively high, in order to minimize grain growth. Pressures below 150 MPa led in all cases to submicrometric or micrometric grain sizes, irrespective of the sintering time and temperature. This was because grain formation takes place from agglomerates in the nanocrystalline powder which neither the milling nor the pressure applied during sintering have eliminated.

(5) In contrast with the microstructured materials which had a homogeneous microstructure, the nanostructured materials did not present a completely homogeneous microstructure since they contained some submicrometric size grains which formed from incompletely eliminated agglomerates in the starting powder.

## Acknowledgements

This work was supported financially by the Ministry of Education and Science (Government of Spain) through Project MAT2006-03068 and by the Junta de Andalucía (Spain) through the Excellency Project P05-0337-FQM. Funding through the Project MAT2010-16848 is also acknowledged.

## References

[1] L. Liu, J.H. Edgar, Substrates for gallium nitride epitaxy, Mater. Sci. Eng. Rep. 37 (2002) 61–127.

[2] A. Can, M. Herrmann, D.S. McLachlan, I. Sigalas, J. Adler, Densification of liquid phase sintered silicon carbide, J. Eur. Soc. 26 (2006) 1707–1713.

[3] Y. Shinoda, T. Nagano, Fabrication of nanograined silicon carbide by ultrahigh-pressure hot isostatic pressing, J. Am. Ceram. Soc. 82 (1999) 771–773.

[4] D.E. Clark, D.C. Folz, What is microwave processing? in: Microwave Solutions for Ceramic Engineers, Am. Ceram. Soc., Inc., Westerville, OH, 2004, pp. 1–34.

[5] H.S. Shulman, M.L. Fall, W.J. Walker, Sintering uniformity and reproductibility with 2.45 GHz, Microwaves in a Industrial Sized Chamber, Presented at 104 Annual Congress of the American Ceramic Society, St. Louis, MO, 2002.

[6] T.A. Baeraky, Microwave measurements of the dielectric properties of silicon carbide at high temperature, Egypt. J. Sol. 25 (2002) 263–273.

[7] S. Mandal, A. Seal, S.K. Dalui, A.K. Dey, S. Ghatak, A.K. Mukhopadhyay, Mechanical characteristics of microwave sintered silicon carbide, Bull. Mater. Sci. 24 (2001) 121–124.

[8] A. Goldstein, W.D. Kaplan, A. Singurindi, Liquid assisted sintering of SiC powders by MW (2.45 GHz) heating, J. Eur. Ceram. Soc. 22 (2002) 1891–1896.

[9] M. Ohyanagi, T. Yamamoto, Consolidation of nanostructured SiC with disorder–order transformation, Scr. Mater. 50 (2004) 111–114.

[10] T. Yamamoto, H. Kitaura, Y. Kodera, T. Ishii, Consolidation of nanostructured β-SiC by spark plasma sintering system, J. Am. Ceram. Soc. 87 (2004) 1436–1441.

[11] F. Guillard, A. Allemand, J.-D. Lulewicz, Densification of SiC by SPS-effects of time, temperature and pressure, J. Eur. Ceram. Soc. 27 (2007) 2725–2728.

[12] Z.-H. Zhang, F.-C. Wang, J. Luo, S.-K. Lee, L. Wang, Processing and characterization of fine-grained monolithic SiC ceramic synthesized by spark plasma sintering, Mater. Sci. Eng. A 527 (2008) 2099–2103.

[13] Z.-G. Yang, L.L. Shaw, Synthesis of nanocrystalline SiC at ambient temperature through high energy reaction milling, Nanostruct. Mater. 7 (1996) 873–886.

[14] X.Y. Yang, Z.W. Huang, Y.K. Wu, H.Q. Ye, HREM observations of the synthesized process of nano-sized SiC by ball milling of Si and C mixed powders, Mater. Sci. Eng. A 300 (2001) 278–283.

[15] D. Chaira, B.K. Mishra, Synthesis and characterization of silicon carbide by reaction milling in a dual-drive planetary mill, Mater. Sci. Eng. A 460–461 (2007) 111–120.

[16] H. Abderrazak, M. Abdellaoui, Synthesis and characterization of nanostructured silicon carbide, Mater. Lett. 62 (2008) 3839–3841.

[17] B. Ghosh, S.K. Pradhan, Microstructural characterization of nanocrystalline SiC synthesized by high-energy-ball-milling, J. Alloys Compd. 486 (2009) 480–485.

[18] B.D. Cullity, Elements of X-ray Diffraction, Addison-Wesley, Boston, 1978

[19] F. Sánchez-Bajo, A.L. Ortiz, F.L. Cumbrera, Analytical formulation of the variance method of line-broadening analysis for voigtian X-ray diffraction peaks, J. Appl. Crystallogr. 39 (2006) 598–600.

[20] A.L. Ortiz, W. Osborn, T. Markmaitree, L.L. Shaw, Crystallite sizes of LiH before and after ball milling and thermal exposure, J. Alloys Compd. 454 (2008) 297–305.

[21] H.P. Klug, L.E. Alexander, X-ray Diffraction Procedures for Polycrystalline and Amorphous Materials, Wiley, New York, 1974.

[22] E.M. Mittemeijer, P. Scardi, Diffraction Analysis of the Microstructure of Materials, Springer-Verlag, Berlin, 2004.

[23] R.L. Synder, J. Fiala, H.J. Burger, Defect and Microstructure Analysis by Diffraction, Oxford University Press, Oxford, 1999.

[24] Z.A. Munir, The effect of electric field and pressure on the synthesis and consolidation of materials: a review of the spark plasma sintering method, J. Mater. Sci. 41 (2006) 763–777.